Mapping boron in silicon solar cells using electron energy-loss spectroscopy

M Duchamp[1], C B Boothroyd[1], A Kovács[1], S Kadkhodazadeh[1], T. Kasama[1], M S Moreno[2], B B Van Aken[3], J-P Barnes[4], M Veillerot[4], S B Newcomb[5], R E Dunin-Borkowski[6-1]

[1] Center for Electron Nanoscopy, Technical University of Denmark, DK-2800 Kongens Lyngby, Denmark

[2] Centro Atómico Bariloche, AR-8400 S. C. de Bariloche, Argentina

[3] ECN Solar Energy, P.O. Box 1, NL-1755 ZG Petten, The Netherlands

[4] CEA-Leti, MINATEC Campus, 17 rue des Martyrs, FR-38054 Grenoble Cedex 9, France

[5] Glebe Laboratories, Newport, Co. Tipperary, Ireland

[6] Institute for Microstructure Research, Forschungszentrum Jülich, D-52425 Jülich, Germany

E-mail: martial.duchamp@cen.dtu.dk

Abstract. Electron energy-loss spectroscopy (EELS) is used to study the B distribution in a p-i-n layered solar cell structure. The boron concentration in the p-doped Si layer is expected to be $\sim 10^{21}\,\mathrm{cm}^{-3}$ and should not exceed $10^{17}\,\mathrm{cm}^{-3}$ in the neighbouring intrinsic layer. We show that B concentrations as low as $3 \times 10^{20}\,\mathrm{cm}^{-3}$ (0.6 at. %) can be measured using EELS. Our measurements are in close agreement with real space *ab-initio* multiple scattering calculations and secondary ion mass spectrometry measurements.

1. Introduction

Thin films of amorphous silicon (a-Si:H) are used as active absorber layers in solar cells deposited on steel foil produced by roll-to-roll processing [1]. In order to improve the efficiency of such solar cells, the nature of the defects that act as charge recombination centres and decrease the internal electric field in the active Si layer needs to be understood. In previous work, B contamination of the active Si layer has been measured using secondary ion mass spectrometry (SIMS) and the efficiency has been shown to improve when the B concentration was reduced [2]. However, the lateral and depth resolution of SIMS are limited to about 100 μm and 5 nm, respectively.

Electron energy-loss spectroscopy (EELS) in the transmission electron microscope (TEM) has nanometre spatial resolution, but the detection of low B concentrations is difficult, especially in Si, because energy-loss near-edge structure (ELNES) from the Si L-edge, caused by scattering of inner-shell electrons to the conduction band, extends from 99 eV to >300 eV and interferes with the B K-edge at 188 eV [3]. By using C_S-corrected scanning (S)TEM EELS, B concentrations of $7 \times 10^{20}\,\mathrm{cm}^{-3}$ have been measured with a 3 nm electron beam [4], while Boothroyd *et al.* detected 0.5 at. % B in Ni_3Al by using an iterative averaging process to reduce channel-to-channel variations in the gain [5].

Here, we measure B concentrations in a-Si:H and a-SiC:H layered samples that are of interest for the development of solar cells. In order to determine the minimum detectable B concentration, we

characterize samples that contain both no B and two different concentrations of B. We examine the Si ELNES and B K-edge structures as a function of B concentration. Our results are compared with SIMS measurements of B content in the same samples.

2. Experimental details

Three Si-based layers were grown using plasma-enhanced chemical vapour deposition on Ag and ZnO layers. Test samples contained 200-nm-thick a-Si:H and a-SiC:H layers that were (i) undoped, (ii) lightly B-doped and (iii) highly B-doped. For comparison, typical solar cell stacking grown on a steel substrate involves the growth of (i) 20 nm p-doped Si, (ii) 300 nm of undoped Si and (iii) 20 nm of lightly B-doped SiC layers. A bright-field (BF) TEM image of a real solar cell sample is shown in Fig 1(a).

Thin film silicon solar cells are typically made on plastic, glass or metallic substrates, making sample preparation for TEM difficult. Here, 100nm-thick-TEM specimens were prepared using focused-ion-beam (FIB) milling and finished with a 5 keV Ga^{2+} beam. EEL spectra were acquired in TEM diffraction mode on an FEI Tecnai T-20 equipped with a LaB_6 electron source and an FEI Titan 80-300 equipped using a field emission electron source, with Gatan Tridiem imaging filters. All measurements were carried out at 120 keV to limit electron beam damage.

At each region of interest, 6 energy-loss spectra that were shifted in energy were acquired. Channel-to-channel gain variations were reduced by using an iterative averaging process that is described in detail elsewhere [5]. In order to minimise shot noise, the exposure time was kept as high as possible without damaging the specimen. For large area measurements, each spectrum was acquired for one minute using a beam diameter of approximately 200 nm in TEM diffraction mode. For higher spatial resolution measurements, line scans were acquired using a 5 nm spot size in TEM diffraction mode. Each spectrum recorded for 1.5s.

Real space multiple scattering calculations were performed using FEFF9 9.05 software, taking into account experimental parameters such as beam energy and collection angle. In order to include core hole effects, the final-state-rule approximation was used. The Hedin-Lundqvist self-energy was used to take inelastic losses into account. Calculations were performed for crystalline SiC and Si. Static disorder of approximately 8 times the Debye-Waller factor was added to simulate amorphous materials. Variations in B concentration were modelled by changing the cluster size (with a small cluster size corresponding to a high B concentration) and/or with different numbers of B atoms replacing Si in different coordination shells. The B K-edge was calculated for concentrations of approximately 0.7 at. % and 2.1 at. % B in Si and SiC.

3. Si L_1 edge ELNES: simulations and experimental data

Ab initio calculations of ELNES from the Si L_1-edge are shown in Fig. 1(b) for crystalline and disordered Si and SiC. Both materials have significant ELNES close to the B K-edge position, which is observed to depend on C concentration. The simulations predict a decrease in ELNES when disorder is included, for both Si and SiC. Fortunately, there is no Si L_1-edge peak exactly at the B K-edge position, making the detection of the B K-edge on top of the Si and SiC L_1 ELNES easier. Figure 1(b) shows that a reasonable match is obtained between the experimental and simulated Si L_1-edge positions, even though the L_{23} contribution is difficult to extract and has an influence on the experimental data. Unfortunately, a simple power-low background-subtraction is difficult due the presence of the strong Si L_1-edge ELNES below 185 eV.
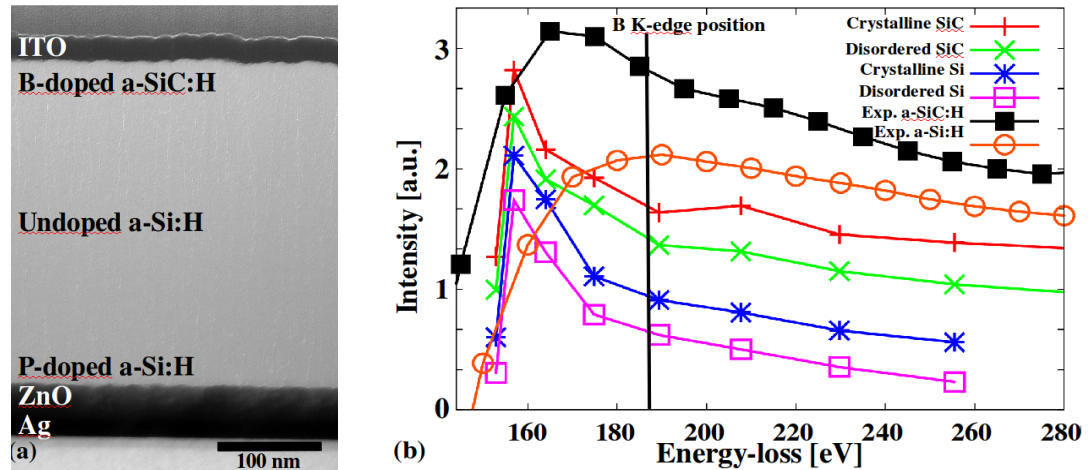
Figure 1. (a) BF TEM image of an a-Si solar cell prepared using FIB milling. (b) Si L_1-edge ELNES calculations for Si and SiC for both crystalline and disordered atomic configurations. Experimental EEL spectra for a-Si:H and a-SiC:H are also shown. The spectra have been shifted vertically for clarity.

4. B K-edge: quantitative analysis

Experimental background-subtracted B K-edge EEL spectra measured from samples containing different B concentrations are shown in Figs 2 (a) and (b). The signals were therefore separated from their backgrounds using a combination of a power law and first order affine functions. The B peaks from highly-doped a-SiC:H and a-Si:H layers are clearly recognisable in Fig 2 and match the simulated B peaks well after refining the crystallinity and cluster size in the simulations. The increase in the intensity of the SiC spectrum at energies higher than 195 eV is due to the Si L_1 ELNES and is consistent with the peak centred at 210 eV found in the calculations (see Fig 1(b)). An energy shift of the lightly doped samples is observed which is not yet understood.
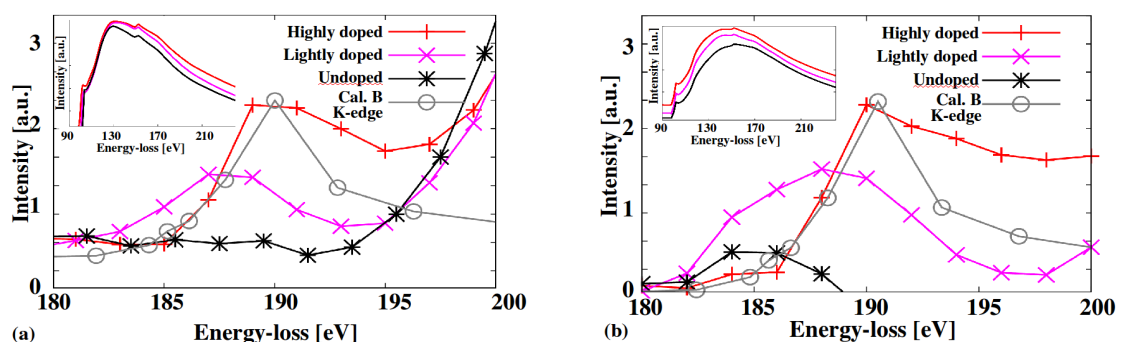

Figure 2. EEL spectra acquired from (a) a-SiC:H and (b) a-Si:H for three different B concentrations. Backgrounds have been subtracted using power law and first order affine functions fitted to the range 175 to 185 eV. The inserts show the spectra before background subtraction of the Si ELNES.

B compositions were determined from the spectra using Hartree-Fock cross-section [6] and are given in Table 1. The relative B concentration obtained by SIMS was estimated by assuming the total number of atoms to be 5×10^{22} cm^{-3}. For the undoped sample, no measurable B was detected using EELS. The lowest B concentration that was measured by EELS with a 200 nm spot size was 0.6 at.%.

Table 1. B and C concentrations in test samples measured by EELS and SIMS

	Si			**SiC**	
	B_{EELS} [%]	B_{SIMS} [%]	C_{EELS} [%]	B_{EELS} [%]	B_{SIMS} [%]
Highly doped	4.74	6	15	1.96	3.04
Lightly doped	1.85	1.4	16.29	0.62	0.6
undoped	0	3.10^{-3}	14.42	0.06	3.10^{-3}

Figure 3 shows the result of an initial attempt to measure B profile with EELS using a 5 nm spot size in an a-SiC:H sample close to the ITO interface, as would be present in a real solar cell. The B concentration measured using EELS is higher than that from SIMS. The discrepancy may be explained by the fact that the SIMS measurements is averaged over large regions.
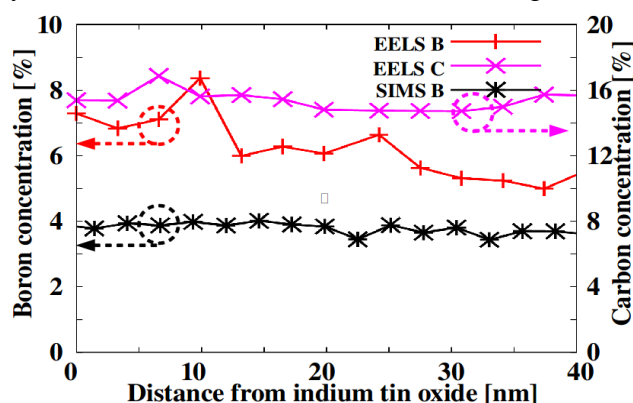

Figure 3. B and C concentrations measured using EELS with a 5 nm spot size. B concentrations measured using SIMS are also shown.

5. Conclusions

B concentrations in a-Si:H and a-SiC:H test structures have been measured using EELS in combination with iterative averaging. Reasonable agreement has been found between SIMS and EELS measurements, within a factor better than 2. B concentrations as low as 0.6 at.% have been measured in a-SiC:H and a detection limit for B of approximately 3×10^{20}cm^{-3} has been estimated for the present experimental parameters. An attempt to measure B concentration profiles by EELS with a 5 nm spot size shows promise for the characterization of a real solar cell sample. Results obtained using other TEM techniques, such as low-loss EELS and off-axis electron holography will be compared with the present approach elsewhere.

References

[1]　Van Aken B B, Dorenkamper M, Devilee C, Heijna M C R, Loffler J and Soppe W J 2009 *34th IEEE photovoltaic specialists conference* **1-3** 426
[2]　Kroll U, Bucher C, Benagli S, Schönbächler I, Meier J, Shah A, Ballutaudb J, Howling A, Hollensteinb Ch, Buchelc A and Poppellercet M 2004 *Thin solid films* **451-452** 525
[3]　Muto S, Sugiyama H, Kimura T and Tanabe T 2004 *Jap. J. Appl. Phys.* **43** 1076
[4]　Asayama K, Hashikawa N, Kajiwara K, Yaguchi T, Konno M and Mori M. 2008 *Appl. Phys. Exp.* **1** 074001
[5]　Boothroyd C B, Sato K and Yamada K 1990 *Proc. XIIth Int. Congress for Electron Microscopy, Seattle, Washington, USA* 80
[6]　Egerton R F 1999 *J. Electron Microscopy* **48** 711